Four-band extended Hubbard Hamiltonian for the one-dimensional cuprate Sr_2CuO_3: Distribution of oxygen holes and its relation to strong intersite Coulomb interaction

R. Neudert, S.-L. Drechsler,* J. Málek,† H. Rosner,‡ M. Kielwein, Z. Hu, M. Knupfer, M. S. Golden, and J. Fink
Institut für Festkörper- und Werkstofforschung Dresden, P.O. Box 27016, D-01171 Dresden, Germany

N. Nücker, M. Merz, and S. Schuppler
Forschungszentrum Karlsruhe, Institut für Nukleare Festkörperphysik, P.O. Box 3640, D-76021 Karlsruhe, Germany

N. Motoyama, H. Eisaki, and S. Uchida
Department of Superconductivity, The University of Tokyo, Bunkyo-ku, Tokyo 113, Japan

M. Domke and G. Kaindl
Institut für Experimentalphysik, Freie Universität Berlin, Arnimallee 14, D-14195 Berlin, Germany

(Received 24 November 1999)

We have carried out experimental and theoretical studies of the unoccupied electronic structure of Sr_2CuO_3, which can be regarded as the best realization of a one-dimensional model system containing cuprate chains. In the polarization-dependent x-ray absorption spectra, the contributions to the upper Hubbard band from states originating from the two inequivalent oxygen sites are energetically well separated. Theoretical analysis of the measured hole distribution within cluster calculations reveals a markedly enhanced effective nearest-neighbor intersite Coulomb interaction, $V_{pd} \sim 2$ to 3 eV, or sizable contributions from next-nearest-neighbor interactions, provided a finite on-site energy difference of the two inequivalent oxygen sites Δ_{pp} is taken into account. Including next-nearest-neighbor interactions, reasonable agreement can be achieved with recent electron energy-loss spectroscopy data from the same compound. The $2p$ oxygen orbital analysis of the unoccupied electronic structure of the single-chain cuprate Sr_2CuO_3 reveals strong similarities with that of the double chain compound $SrCuO_2$.

I. INTRODUCTION

Quasi-one-dimensional (1D) cuprate compounds are model systems allowing experimental access to a number of basic physical phenomena in low dimensions, such as spin-charge separation[1,2] or the existence of a spin gap in ladder materials depending on the number of legs.[3] Among the extensive cuprate family, which is based upon compounds with Cu^{2+} ions in a fourfold coordinated oxygen environment (the planar CuO_4 plaquette), the single chain built up of corner-shared CuO_4 plaquettes (''corner-shared linear chain''), most ideally realized in Sr_2CuO_3, plays an important role, as it is the basic structural element of more complex systems like the double chain in $SrCuO_2$ and the ladder-type structures. Figure 1 shows the crystal structure of Sr_2CuO_3 and $SrCuO_2$.

At temperatures above 20 K Sr_2CuO_3 is the best known realization of a spin-$\frac{1}{2}$ antiferromagnetic Heisenberg chain,[4–6] showing what is possibly a record value for the nearest-neighbor exchange integral $J \approx 200$ to 250 meV, which significantly exceeds the corresponding values in the 2D cuprates of 130 to 150 meV. The microscopic origin for this unexpected high J value remains unclear at present[7] and its elucidation requires a detailed knowledge of the underlying electronic structure of the chain cuprates.

From the electronic point of view there is also considerable general interest in comparing Sr_2CuO_3 with other members of the growing cuprate family, especially with the parent compounds of the layered high-T_c superconductors. These parent compounds are typical charge transfer insula-

tors within the classification of Zaanen, Sawatzky, and Allen.[8] Interpreting various experimental or theoretical data several authors have claimed that Sr_2CuO_3 is *different*, exhibiting, for instance, a significantly reduced charge transfer energy $\Delta_{pd} = 0.5$ to 2.5 eV,[9] derived from valence band pho-
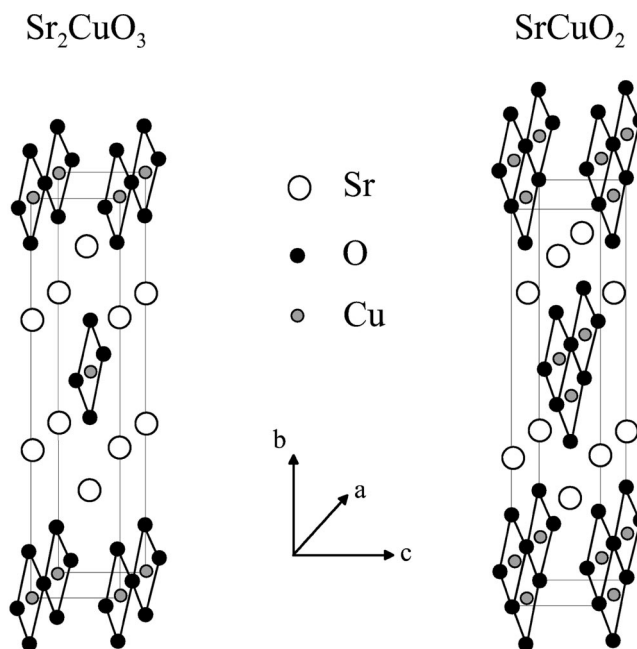

FIG. 1. Crystal structures of the linear chain cuprates Sr_2CuO_3 (left) and $SrCuO_2$ (right). The corner-shared single and double chains are running along the direction of the a axis.

toemission data and Cu $2p$ core-level x-ray photoemission spectra (XPS), to be compared with 3.5 to 4 eV for typical 2D cuprates.[10] In order to reproduce the value of the experimental charge transfer gap $E_g = 1.5 \pm 0.3$ eV derived from He I ultraviolet photoemission combined with bremsstrahlung isochromat spectroscopy[9] of Sr_2CuO_3, a significantly enhanced nearest-neighbor intersite Coulomb interaction $V_{pd} \sim 2$ eV has been suggested.[10] Unfortunately, the Cu $2p$ XPS is rather insensitive to the actual value of V_{pd} and to the best of our knowledge its magnitude has not been estimated, at least semiquantitatively, from experimental data for any other cuprate compound, except the rough estimate of Eskes *et al.*[11] based on various spectroscopic data of 2D and 3D cuprates, which yields $V_{pd} < 1$ eV. These relatively small values should be compared with various theoretical values of unscreened and screened interactions for the CuO_2 plane. In the ''unscreened'' case $V_{pd} \sim 4$ to 6 eV has been estimated by Stechel and Jennison[12] and Rushan *et al.*,[13] respectively, and $V_{pd} \sim 1$ to 3 eV in the more realistic ''screened'' case.[13] Furthermore, $V_{pd} \approx 0.8 \pm 0.25$ eV and 1.2 ± 0.5 eV has been obtained by McMahan *et al.*[14] and Hybertsen *et al.*,[15,16] respectively, from constrained local density approximation (LDA) calculations for La_2CuO_4. For the oxygen-oxygen intersite Coulomb interaction $V_{pp} \approx 0.7$ to 2 eV was estimated in Ref. 12, while a negligibly small value $V_{pp} < 0.7$ eV within error bars was stated in Ref. 15.

In general, knowledge of the intersite Coulomb interaction is of interest for any quantitative realistic description of cuprate physics. Moreover, it is a key quantity for the charge transfer between CuO_3 chains and CuO_2 planes in the $RBa_2Cu_3O_{6+\delta}$ high-T_c superconductors,[17] as well as for various possible charge density instabilities and related phase separation scenarios induced by doping of the parent charge transfer insulators.[18] Naturally, the binding energy of excitons in insulating cuprates is sensitive to the magnitude of the intersite Coulomb interaction.[19]

Returning to Sr_2CuO_3, we note that a strongly enhanced nearest-neighbor Coulomb interaction $V^{(1B)} = 0.8$ eV as well as a moderately enhanced transfer integral $t^{(1B)} = 0.55$ eV in the context of a 1D extended one-band (1B) Hubbard model have been deduced from recent electron energy-loss spectroscopic (EELS) data.[20] The corresponding theoretical values for the 2D CuO_2 plane derived for La_2CuO_4, which has even smaller Cu-O bond lengths ($d = 1.89$ Å) than Sr_2CuO_3 ($d = 1.95$ Å) are $V_{2D} = 0.11$ to 0.14 eV,[14,21] and $t_{2D} = 0.42$ to 0.48 eV.[14,16] For the corresponding single-band extended tight binding model, the same enhanced value of the nearest-neighbor transfer integral as derived from the EELS data mentioned above was predicted from LDA linear combination of atomic orbitals (LCAO) band structure calculations.[22] Recent angle resolved photoemission measurements of Sr_2CuO_3 yield $t^{(1B)} \sim 0.5$ eV from the width of the holon dispersion.[2]

In this paper we present a polarization-dependent x-ray absorption spectroscopic (XAS) study of the unoccupied electronic structure of Sr_2CuO_3, which we combine with an appropriate theoretical analysis in order to set constraints on the parameter values mentioned above. A similar XAS study was performed recently on the related double-chain (''zigzag'') compound $SrCuO_2$,[23] and we will show that discus-

sion of the hole distribution of both chain geometries is possible within one consistent picture. Furthermore, we relate our results obtained from XAS to the values deduced from EELS within an extended one-band Hubbard model,[20] since both experiments are highly sensitive to the effect of intersite Coulomb interactions.

The paper is organized as follows. In Sec. II the experimental techniques and sample handling as well as the theoretical approaches, using mainly exact diagonalization studies of small clusters within the pd model, are outlined. The experimental results are presented in Sec. III. The theoretical interpretation of the O $1s$ XAS data is given in the context of various dp model parameter sets in Sec. IV. In order to get additional insight into the interdependencies of various onsite and off-site interaction parameter values and their possible bounds, we compare our findings with the recent single-band analysis of the EELS data of Sr_2CuO_3 in Sec. V. For this purpose we have also included an Appendix which contains an approximate expression for the effective on-site repulsion of the single-band extended Hubbard model in terms of the four-band dp model and also discusses the limitations in its use. Finally, in Sec. VI we compare our results with the O $1s$ XAS data of the related double-chain compound $SrCuO_2$ which is analyzed briefly in the asymmetric dp model, before a summary is given in Sec. VII.

II. METHODS

A. Experiment

Single crystals were grown using the traveling-solvent-zone technique.[5] Sr_2CuO_3 adopts an orthorhombic crystal structure with lattice parameters $a = 3.91$ Å, $b = 12.71$ Å, $c = 3.50$ Å.[24] Note that we have interchanged the notation of the axes with respect to Ref. 24 for the convenience of the reader so as to be able to use the same orbital notation for both this chain system and the layered cuprates. Following our convention, the chain direction lies now along the **a** (x) direction [see Fig. 1] and the **c** (z) direction is perpendicular to the planar CuO_4 plaquettes. Although the Cu-O distances in **a** and **b** directions are almost identical, the different site symmetries of the central oxygen sites O(1) and the peripheral oxygen sites O(2) should be kept in mind. The orientation of the crystals was determined using x-ray diffraction.

The XAS experiments were carried out using the SX700/II beam line[25] operated by the Freie Universität Berlin at the BESSY synchrotron radiation source (Berlin) using linearly polarized light. The energy resolution of the monochromator was set to be 280 and 660 meV at the O $1s$ and Cu $2p$ absorption thresholds, respectively.

The crystals are extremely sensitive to exposure to atmospheric moisture. In test measurements on *ex situ* prepared samples, surface effects have been observed even in the ''bulk'' sensitive fluorescence yield detection mode, which has a probing depth of several tenths of a micrometer. To avoid these difficulties we have performed our measurements on freshly cleaved samples at a base pressure of 5×10^{-10} mbar. For the O $1s$ and Cu $2p$ absorption spectra we chose the fluorescence yield (FY) and total electron yield (TEY) detection modes, respectively.[26] Energy calibration was performed by comparison of the Cu $2p_{3/2}$ XAS signal of a CuO sample with corresponding data in the literature.[27] In

all cases the data were corrected for the energy dependent incident photon flux and, in the case of O 1s, for self-absorption effects, following a procedure described elsewhere.[28] The spectra for different crystal orientations are normalized ~ 80 eV above the absorption threshold, where the final states are nearly free-electron-like and therefore essentially isotropic.

XAS is a well-established method to investigate the character and the symmetry of the unoccupied electronic states in cuprate-based materials.[29] As dipole selection rules apply and due to the localized initial core states, our studies probe the site specific hole distribution, i.e., unoccupied O 2p and Cu 3d/4s final states in the case of O 1s and Cu 2p absorption, respectively.[30] In addition, by using linearly polarized synchrotron radiation and single-crystalline samples it is possible to select further the transitions with different symmetry into the 2p O and 3d Cu orbitals, by orienting the sample with respect to the electric field vector **E** of the incoming light. For example, in the geometry **E**$\|$**a** only O 1s $\rightarrow$O 2p_x transitions are possible. The crystals cleave in the (ac) plane, i.e., it is necessary to extrapolate the spectra for **E**$\|$**b** from measurements at grazing incidence (70° from the sample surface normal).

B. Theoretical description: From LDA calculations to the four-band dp extended Hubbard model

To get some first insight into the electronic structure we have performed LDA-LCAO (and linear muffin tin orbital) band structure calculations for Sr$_2$CuO$_3$ with a minimum basis, treating the Cu (4s,4p,3d) O (2s,2p), and Sr (5s,5p,4d) orbitals as valence states and the lower states as core states. In comparison with our previous work,[22] the accuracy of the Madelung potential construction has been improved here, resulting in slightly narrower bandwidths of the valence bands (the Cu 3d/O 2p band complex).

Three orbitals contribute more than 94% of the total net density of states (DOS) of the half-filled antibonding band crossing the Fermi energy, namely, the O 2p_x and O 2p_y as well as the Cu 3$d_{x^2-y^2}$, as expected from simple chemical bonding considerations. Hence, the standard dp model with the inclusion of two nonequivalent oxygen sites per unit cell can be regarded as a quite good starting point for the description of this compound's low-energy electronic structure. With four atoms per unit cell and one orbital per site [Cu 3$d_{x^2-y^2}$, 2×O(2) 2p_y, and O(1) 2p_x; see Fig. 2] we arrive at the standard four-band extended Hubbard model (see, for instance, Refs. 31 and 32):

$$H = \sum_i \varepsilon_i \hat{n}_i + \sum_{\langle i,j\rangle,s} t_{ij}(c_{i,s}^\dagger c_{j,s} + \text{H.c.}) + \sum_i U_i \hat{n}_{i,\uparrow}\hat{n}_{i,\downarrow}$$

$$+ \sum_{\langle i,j\rangle} V_{ij}\hat{n}_i\hat{n}_j, \tag{1}$$

where $c_{i,s}^\dagger$ creates a hole with spin projection $\pm 1/2$ at site i, $\hat{n}_{i,s} = c_{is}^\dagger c_{is}$ denotes the number operator, and $\hat{n}_i = \sum_s c_{is}^\dagger c_{is}$. The symbol $\langle i,j\rangle$ denotes the summation over nearest-neighbor (NN) bonds including also the bond between O(1) and O(2). In the hole picture adopted here the vacuum state of the Hamiltonian Eq. (1) is given by the electronic
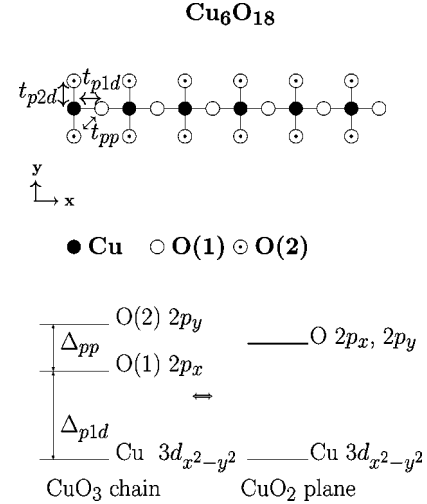
Cu|3$d^{10}\rangle$ O|2$p^6\rangle$ configuration. Thus one deals with an occupancy of one hole per CuO$_3$ unit. In the present paper we shall restrict ourselves to consideration of the strongly correlated ground state of Sr$_2$CuO$_3$.

It is impossible to extract all (from 8 to 12) Hamiltonian parameters from the O 1s XAS data alone. To circumvent this difficulty, we shall adopt several parameters suggested by the analysis of recent complementary XPS, XAS, and EELS studies. We include also the LDA-LCAO results mentioned above since, according to our experience for numerous cuprates, this calculation yields quite reasonable values of the transfer integrals.[33] Here we will try (i) to elucidate to which parameters of the Hamiltonian given by Eq. (1) the physical quantities measured by O 1s XAS are in principle most sensitive and (ii) to find interdependencies for them set by the present data. The qualitative effect of the intersite Coulomb interaction upon the relative hole densities at the two inequivalent oxygen sites, generic for corner-shared cuprate chains, will be shown to be the same for quite distinct sets of transfer integrals. The parameter sets that are discussed within this paper are summarized in Table I.

For the transfer integrals t_{ij} we use the same sign convention as in Ref. 37. However, concerning their magnitude, enhanced oxygen-copper transfer integrals can be expected from the large value of the exchange integral J mentioned in the Introduction. The LDA calculations point to the same tendency: $t_{p1d}=1.45$ eV, $t_{p2d}=1.8$ eV compared with 1.3 eV for typical layered cuprates, where t_{p1d} and t_{p2d} denote the oxygen O(1)-copper and the oxygen O(2)-copper transfer integrals, respectively (see set I in Table I). The unusually large value for the oxygen-oxygen transfer integral $t_{p1p2} \equiv t_{pp}=1.15$ eV derived from our LDA-LCAO calculations within a straightforward four-band fit can be attributed to difficulties in the unique assignment of a dispersive ''nonbonding'' band in different parts of the Brillouin zone. Alternatively, a fit of the whole planar pd band complex within

FIG. 2. A sketch of the cluster type modeling the CuO$_3$ chains shown in Fig. 1, of the transfer integrals, and of the on-site energies of the pd Hamiltonian [Eq. (1)] adopted in the present work. Upper half: Type of periodic clusters considered in the present paper. For the magnitudes and the signs of the transfer integrals t_{ij} see the text and Table I. Lower half: Schematic view of the on-site energies and the crystal field effect on the inequivalent oxygen sites.

TABLE I. Proposed dp model parameters for Sr_2CuO_3 examined in the present work. All energies are given in eV.

Quantity	KO[a]	Present work (I–III)[b]	TM[c]
		Set	
t_{p1d}	1.3	1.45	0.95
t_{p2d}	1.3	1.8	0.95
t_{pp}	0.65	1.15(I), 0.75(II,III)	0.4
Δ_{p1d}	2.5	3.0	2.39
Δ_{pp}	0	0.5(I,II), 0.75(III)	0.0
U_d	8.8	8.8	8.5
U_p	4.4(I–III) to 6(III)	4.4	4.1
V_{pd}	1.76 to 2.64	2.5(I), 1.9(II), 2.35(III)	0
V_{pp}	0	0(I), 1.35(II), 1.5(III)	0
V_{dd}	0	0 to 0.85 (III)	0

[a]Cu $2p$ XPS, Kotani and Okada (KO1–KO3), Ref. 10.
[b]LDA+O $1s$ XAS, present work.
[c]Tohyama and Maekawa (TM), Ref. 38.

the extended planar $(Cu_{3d}-O_{2p})_{\sigma\text{-}\pi}$ model (containing seven bands, i.e., now with *two* oxygen orbitals $2p_{x,y}$ per site) reveals similar Cu-O transfer integrals but markedly reduced values for the corresponding O(1)-O(2) transfer integrals, $t_{pp}=0.62$ eV and $\tilde{t}_{pp}\sim0.42$ eV for the O(1)-O(2) transfer integral between π bonded oxygen orbitals (O $2p$ lobes far from Cu). As we will see in our analysis, this significantly smaller t_{pp} value derived from the seven-band fit seems to us more appropriate to be used in the four-band extended Hubbard model under consideration since it lowers the value of the exchange integral J toward the value suggested by the experimental data.

In the following we denote the difference between the central oxygen O(1) $2p_x$ and the Cu $3d_{x^2-y^2}$ on-site energies by $\Delta_{p1d}=\varepsilon_{p1}-\varepsilon_d$ and the corresponding difference between the outer oxygen O(2) $2p_y$ and the central oxygen O(1) $2p_x$ on-site energies by $\Delta_{pp}=\varepsilon_{p2}-\varepsilon_{p1}$ (see Fig. 2). For the on-site Coulomb repulsion at Cu and O sites we adopt $U_d=2U_p=8.8$ eV and $U_{p1}=U_{p2}=U_p$, respectively, as suggested by Okada and Kotani.[10] A similar Cu $3d_{x^2-y^2}$ value of $U_d=8.5\pm0.3$ eV has also been proposed for Sr_2CuO_3 by Maiti *et al.*[9] For the nearest-neighbor intersite Coulomb interactions we adopt for the sake of simplicity $V_{p1d}=V_{p2d}=V_{pd}$. To illustrate the effect of V_{pd} we will also examine parameter sets where this interaction has not been considered.[38,39] Finally, we will also consider the effect of next-nearest-neighbor (NNN) intersite Coulomb interaction of two holes residing on two neighboring different oxygen sites, V_{pp}, or on the neighboring Cu sites, V_{dd}.

Performing exact diagonalization studies of the Hamiltonian given by Eq. (1) on periodic $(CuO_3)_N$ clusters ($N=2$ to 6) (Fig. 2), we have calculated the hole occupation numbers (expectation values of the number operators)

$$n_i=\langle G|\hat{n}_i|G\rangle, \qquad (2)$$

in the ground state $|G\rangle$ on Cu, n_d, and on both inequivalent oxygen sites O(1) and O(2), n_{p1} and n_{p2}, respectively. The corresponding on-site correlation functions

$$D_i=\langle G|\hat{n}_{i,\uparrow}\hat{n}_{i\downarrow}|G\rangle,$$

describe the small but finite double occupancy which is often neglected in other approximations for the pd Hubbard models. The corresponding NN density-density intersite correlation functions $\langle G|n_in_j|G\rangle$ are abbreviated by $\langle n_dn_{p1}\rangle$, $\langle n_dn_{p2}\rangle$, and $\langle n_{p1}n_{p2}\rangle$.

In the following we exploit the fact that the total integrated weight of the XAS spectral function[16] (up to a normalization factor given by the square of the modulus of the nearly constant transition matrix element) equals the corresponding occupation numbers of holes in the ground state. We emphasize that (i) by definition the integrated weight of this spectral function does not depend on the Coulomb interaction with the core hole and (ii) direct evaluation of this spectral function shows that for the case of an undoped charge transfer insulator under consideration and for typical parameter sets more than 95% of its spectral weight is located within a narrow energy interval of about 1 eV just above the threshold. After broadening with the experimental resolution we are left essentially with a single peak (not shown). Only the peak position is affected by the Coulomb interaction with the core hole, and by the large core-level energy, which in the case of nonequivalent oxygen ions depends on the site where the XAS process takes place. In this context vibrational effects in the final state can be ignored. Furthermore, we neglect possible changes in the Hamiltonian parameters in the vicinity of the excited ion. Thus the measured polarization-dependent O $1s$ XAS spectral weights near the onset probe the oxygen occupation numbers of the corresponding O $2p$ states in the ground state. The value of V_{pd} can then be determined by fitting the XAS data reported below, if the second essentially unknown parameter Δ_{pp} can be obtained from the same data or by other considerations.

For the rating of various parameter sets proposed for Sr_2CuO_3 we will use also the exchange integral J obtained from the mapping of Eq. (1) onto the equivalent antiferromagnetic spin-1/2 Heisenberg model (comparing the triplet-singlet separations[31]) and the value of the charge transfer gap calculated from the well-known relation

$$E_g=E_0[+e]+E_0[-e]-2E_0, \qquad (3)$$

where $E_0[\pm e]$ denote the ground state energy for clusters with one added (subtracted) positive elementary charge.

In order to complement our exact diagonalization studies of periodic rings and to improve the estimation of the related inevitable finite size effects, we have also applied the recently developed efficient incremental technique[40] to calculate the charge gap E_g and the occupation numbers n_i. For this purpose a comparison with available quantum Monte Carlo (QMC) calculations is very illuminating since by QMC techniques significantly larger cluster sizes can be handled, although only approximately.[41–43]

III. EXPERIMENTAL RESULTS (XAS)

A. Cu $2p$ absorption edges

Figure 3 shows the polarization-dependent Cu $2p_{3/2}$ x-ray absorption spectra of Sr_2CuO_3 along all three crystallographic directions. These measurements probe essentially Cu $3d$ final states. All of the Cu $2p$ absorption spectra show a
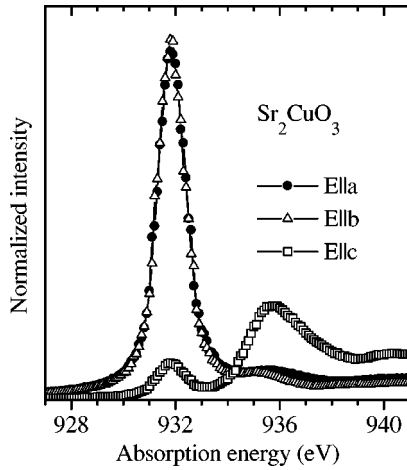
FIG. 3. Cu $2p_{3/2}$ absorption edges of Sr_2CuO_3 for the electric field vector **E** parallel to the three crystallographic axes (Ref. 70).

FIG. 4. O $1s$ absorption edges of Sr_2CuO_3 for the electric field vector **E** parallel to the three crystallographic axes (Ref. 70).

narrow peak at ~ 931.8 eV (the so called white line), which is associated with the Cu $3d$ contributions to the upper Hubbard band (UHB).[29] In accord with the symmetry of the Cu $3d_{x^2-y^2}$ orbital, identical spectra for **E**$\|$**a** and **E**$\|$**b** are observed within the experimental accuracy. In the following, we denote the **E**$\|$**a** and **E**$\|$**b** geometries collectively as in plane. In contrast, a much reduced intensity is found for light polarization perpendicular to the CuO_4 units (**E**$\|$**c**, out-of-plane geometry). The strong anisotropy between the in-plane and out-of-plane geometries reveals that the UHB is predominantly built up of Cu $3d_{x^2-y^2}$ orbitals, while out-of-plane orbitals (Cu $3d_{z^2-r^2}$) contribute less than 5%.[44] Due to deviations from perfectly linear light polarization this value represents an upper limit.

The planar character of the hole states is well known from the 2D cuprates[29,45] and has also been observed in the double-chain compound $SrCuO_2$.[23] To obtain the analogous result for the present case, although not surprising, is still of considerable importance since this confirms that we can restrict the cluster calculations reported below for this chain compound in a good approximation to in-plane orbitals only.

Besides the white line, a strongly polarization-dependent absorption feature is found at 935.8 eV. Features in this energy range in the out-of-plane geometry have been observed in many other cuprates[29] and analyzed in detail in the 2D model system $Sr_2CuO_2Cl_2$. In the latter, a comparison with the calculated density of states showed that this structure is related to transitions into Cu $3d_{3z^2-r^2}$ orbitals which become partly unoccupied via hybridization with empty Cu $4s$ states.[45]

B. O $1s$ absorption edges

We will now turn to the hole distribution between the oxygen sites, where, in contrast to copper, two inequivalent sites are present. The polarization-dependent O $1s$ absorption edges are shown in Fig. 4. The features below 530.5 eV can be regarded as resulting from hybridization of O $2p$ orbitals with the (predominantly) Cu $3d_{x^2-y^2}$ UHB, and will be analyzed in detail below by the dp model introduced above in Sec. II B. The features at higher absorption energies are not included in our quantitative analysis because they
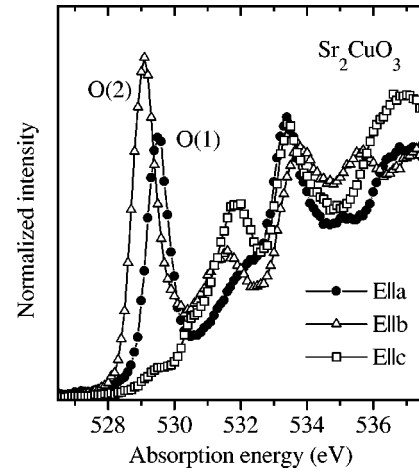
result mainly from the out-of-plane orbital O $2p_z$ or from the hybridization of the orbitals Cu $3d_{x^2-y^2}$, O(1) $2p_x$, and O(2) $2p_y$ with Cu $4s, 3d_{xy}, 3d_{3z^2-r^2}$ states, and are thus not accounted for in the standard dp model.[46]

Returning to the O $2p$ contribution to the UHB near 529.5 eV, the small fraction of holes (less than 5%) observed in the out-of-plane geometry attests to the highly planar character of these oxygen hole states, which predominantly occupy O $2p_x$ and O $2p_y$ orbitals. (The remaining finite value is mainly attributed to the experimentally available slightly nonideal polarization in the present XAS experiment.)

When comparing the spectra for the two in-plane measurements, differences in energy position and spectral weight are observed: for **E**$\|$**a** the UHB derived feature is centered at 529.6 eV, whereas for **E**$\|$**b** it is found at 529.1 eV. One can clearly ascribe the two different peaks to the two symmetrically inequivalent oxygen sites. The O(1) site has two adjacent Cu atoms in the **a** (x) direction, whereas the O(2) site has only one Cu neighbor along the **b** (y) axis. Assuming σ-bonded O orbitals, for **E**$\|$**a** only O(1) $1s \rightarrow$ O(1) $2p_x$ transitions occur, while for **E**$\|$**b** O(2) $1s \rightarrow$ O(2) $2p_y$ transitions are expected. Hence it is possible to assign the energetically lower peak to transitions into unoccupied states at the two O(2) sites and the higher-lying peak to transitions at O(1). A relative hole distribution of approximately 45% at the O(1) and 55% at the two O(2) sites is found, thus slightly favoring the peripheral oxygen sites (in total) for hole occupation. According to our cluster calculations for the XAS spectral density, it turned out that for equal O $1s$ core levels the UHB derived peak for O(2) occurs at lower energies than the peak for O(1), in qualitative agreement with the experimental data. However, the calculated energy difference of about 1.5 eV exceeds the experimentally observed value 0.5 eV. In addition, it depends only weakly on the actual Δ_{pp} value and other model parameters. Therefore the energy difference between the two UHB derived peaks of O(1) and O(2) should be related at least partially to different binding (site) energies of the O $1s$ core levels at the two nonequivalent sites, i.e., the crystal field affects the O $1s$ core levels. In fact, Madelung potentials for Sr_2CuO_3 calculated in the ionic charge model[47–49] show a difference of about 1.98 to 2.07 eV for the sites under consideration. Adopting an isotropic ''screening''

factor of about 2, we would arrive at the experimentally observed value of 0.5 eV in the peak position difference. A more detailed theoretical investigation of this topic including additional LDA calculations is postponed for future work.[50] Similar energy shifts have been observed in $R Ba_2 Cu_3 O_7$ ($R=$ Y,Pr),[53,54] and $Y Ba_2 Cu_4 O_8$,[55] for the doping induced peaks near 528 eV related to the corresponding two oxygen sites of the CuO_3 chains as well as in the double chains[23] in $SrCuO_2$ for the contributions of O(2) derived $2p_y$ states and O(1) derived $2p_{x,y}$ states, respectively, to the upper Hubbard band as found here. In contrast, for the edge-shared compounds $Li_2 CuO_2$ (Ref. 56) and $CuGeO_3$ (which have only equivalent oxygen sites involved in the CuO_4 plaquette) significantly smaller shifts of 0.15 eV and 0.1 eV, respectively, have been detected for polarizations perpendicular and parallel to the chain direction.

IV. DISCUSSION OF VARIOUS *dp* MODEL SETS WITH RESPECT TO THE XAS RESULTS

In the following we denote the relative oxygen hole distribution in $Sr_2 CuO_3$ by the factor

$$R_{XAS} = 2n_{p2}/n_{p1} = 1.22 \pm 0.1,$$

as obtained from our O $1s$ XAS measurements. Within a simple hybridization picture neglecting different on-site energies of the two nonequivalent oxygens, one might expect $R \approx 1$ since the $2p_y$ orbital of O(2) has only one Cu neighbor to overlap, while the $2p_x$ orbital belonging to O(1) has two Cu neighbors. Notice that the LDA results in a significantly larger value of $R = 1.66$ by integrating the orbital resolved net densities of states from E_F up to the top of the antibonding band. This indicates, in addition to the absence of the charge transfer gap within the LDA, the necessity of taking more electron correlation effects into account, as is done within our theoretical approach.

A. Examination of parameter sets for $Sr_2 CuO_3$ proposed in the literature

1. Parameter set TM: No intersite Coulomb interaction and equal oxygen on-site energies

Let us start with examination of the simplest possible parameter set in which the intersite Coulomb interaction is ignored and $\Delta_{pp} = 0$ (see Table I). Such a set, proposed by Tohyama and Maekawa (TM),[38,39] was originally conceived to describe the optical conductivity of the layered cuprates $Nd_2 CuO_4$ and $La_2 CuO_4$. $Nd_2 CuO_4$ exhibits similar Cu-O distances as $Sr_2 CuO_3$ and a planar structure without any buckling of the Cu-O bonds. It has also a similar optical gap of about 1.5 eV as well as no apical oxygen ion(s) residing above and/or below the CuO_4 plaquette. Note that the TM transfer integrals are very small (see Table I). In Ref. 10 it has been shown that such a set does not describe the Cu $2p$ XPS data either for $La_2 CuO_4$ or for $Sr_2 CuO_3$. Here we shall show that the same holds also with respect to our O $1s$ XAS and the EELS data.

In fact, taking the TM parameters, we arrive at $R_{TM} \approx 0.93$ which is significantly smaller than our experimental value $R_{XAS} = 1.22$. Note that by adding a moderate intersite
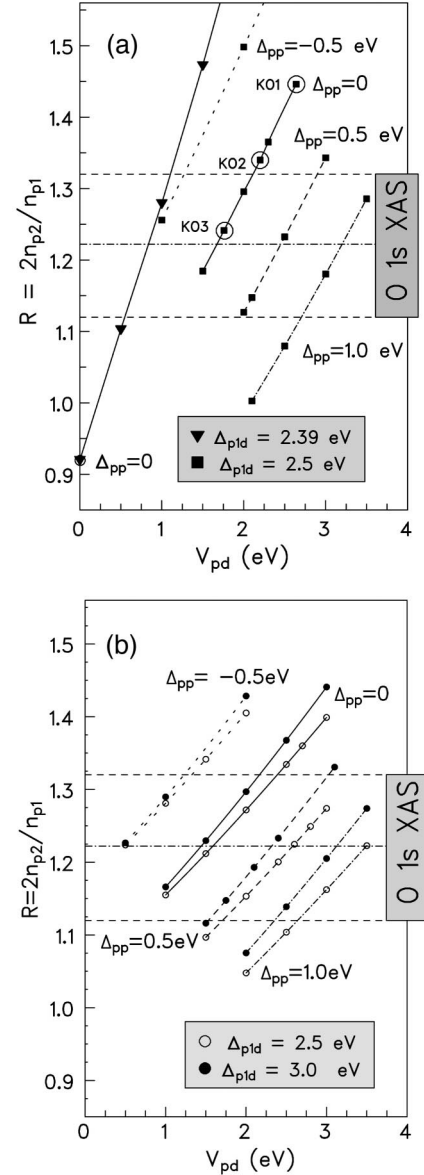

FIG. 5. The relative hole distribution between the two inequivalent oxygen sites $R = 2n_{p2}/n_{p1}$ for different on-site energies Δ_{p1d} and Δ_{pp} explained in the text and shown schematically in Fig. 2, vs intersite Coulomb interaction V_{pd}. The experimental values derived from the O $1s$ XAS data shown in Fig. 4, including the error bars, are given by the stripe in the middle of the figures. (a) For the TM parameter set extended by variable V_{pd} (triangles) (the original TM parameter set is marked by a circle) and analogously for the KO sets (KO1 to KO3, squares; full line) extended to different NN Coulomb interactions V_{pd} *and* to different on-site energies of both oxygen sites measured by Δ_{pp} (dashed, dotted, and dash-dotted curves). The original parameter sets KO1 to KO3 are marked by circles and display the V_{pd} interval $V_{pd} = (0.2 \text{ to } 0.3)U_d$ recommended in Ref. 10. (b) The same for parameter set I explained in Table I.

Coulomb interaction $V_{pd} \sim 1$ eV, the situation with respect to XAS can be significantly improved. This is illustrated in Fig. 5(a), where we have extended the original TM parameter set to finite values of V_{pd}. However, difficulties with respect to the underestimation of the charge gap and/or with respect to the single-band parameters derived from the EELS

data as well as the value of the exchange integral do remain (see below).

2. Parameter sets KO: NN intersite Coulomb interaction included, but with equal oxygen on-site energies

Next we examine the parameter set suggested by Okada and Kotani (KO) (see Table I).[10] The essential approximations made therein are (i) neglect of the inequivalence of the two oxygens, $t_{p1d} = t_{p2d} = 1.3$ eV, $t_{pp} = 0.65$ eV, $\Delta_{pp} = 0$, so that the transfer integrals are taken as for layered cuprates but for (ii) a reduced charge transfer energy $\Delta_{p1d} = 2.5$ eV, and (iii) a strongly enhanced nearest neighbor intersite Coulomb interaction $V_{pd} = 0.2U_d$ to $0.3U_{dd}$. Below we will examine in detail the proposed range of $V_{pd} = 0.3U_d$ (set KO1), $0.25U_d$ (set KO2), and $0.2U_d$ (set KO3) while fixing the remaining parameters.

For the periodic Cu_4O_{12} cluster and $V_{pd} = 2.64$ eV (KO1), our value for the Cu occupation number of $n_d = 0.6079$ reproduces well their reported value of 0.608. However, inspection of the results from the Cu_6O_{18} cluster shows that there remain finite size effects resulting in a slightly reduced charge at the Cu site, $n_d = 0.596$. Since the difference charge is now localized to a large extent at the inner oxygen O(1), which exhibits a smaller hole density of $n_{p1} = 0.165$, the oxygen hole ratio R_{calc} (measuring the relative distribution) is somewhat more strongly reduced from $R = 1.5198$ to $R = 1.4461$ on going from a four- to a six-copper-site cluster. As has been discussed in Sec. II B the last quantity is already rather close to the infinite chain limit. The three KO parameter sets are included in the R vs V_{pd} plot shown in Fig. 5(a). The set KO1 with identical central and outer oxygen on-site energies *and* with the strongest intersite Coulomb energy of $V_{pd} \sim 0.3U_{dd}$ clearly overestimates the value of R_{XAS} although it is closer than the original TM set discussed above. Their next, intermediate, set (KO2) with $V_{pd} = 0.25U_d = 2.2$ eV [for which in Ref. 10 the superexchange integral $J \approx 200$ meV has been estimated from a Cu_2O_7 (open) cluster] yields $R = 1.34$, which lies slightly above our XAS error bars. Only their lowest set KO3 with $V_{pd} = 1.76$ eV would be in reasonable agreement with our XAS data. Some disadvantages of this and the intermediate set KO2 with respect to the EELS data and the charge transfer gap E_g are discussed below. Figure 5(a) also contains an extension of the original KO parameter sets ($\Delta_{pp} = 0$) to finite values of Δ_{pp} to illustrate the influence of this on the calculated R value. In general, a larger Δ_{pp} has to be compensated by an increased V_{pd} to reproduce the experimentally observed hole distribution [see Eq. (5)].

B. Present approach: Inequivalent oxygen sites vs intersite Coulomb interaction

Generally speaking, there is no reason to assume that (i) the on-site energies of both oxygen sites in Sr_2CuO_3 should coincide and (ii) once strongly enhanced NN intersite Coulomb interactions are present, at the same time NNN interactions will be negligible. Both of these points will be considered in more detail below. In this context we mention with respect to (i) that, for the CuO_3 chains in $YBa_2Cu_3O_7$, significantly large values of Δ_{pp} have been found. $\Delta_{pp} = 2 \pm 0.5$ eV has been obtained from simulation of the O $1s$

XAS data of Nücker *et al.*[53] within a standard dp ''CuO_2-plane-like'' parameter set adopting $V_{pd} \sim 1$ eV and $V_{pp} \sim 0.5$ eV.[31] $\Delta_{pp} = 2.4$ eV has been extracted from simulation of the charge transfer between CuO_3 chains and CuO_2 planes as well as the oxygen ordering in the basal plane,[57] and $\Delta_{pp} \sim 2V_{pd}$ has been obtained with the constraint $0.74t_{pd} < 2V_{pd} < 2.6t_{pd}$.[17] With these independent results in mind one can expect $\Delta_{pp} > 0$ for the present case, too. However, as will be discussed below, large values of Δ_{pp} of the order of ~ 2 eV can be excluded for Sr_2CuO_3.

The calculated oxygen hole ratio R as a function of V_{pd} is presented in Fig. 5(b) for our LDA LCAO derived parameter set (I) with various values of Δ_{p1d} and Δ_{pp}. With increasing V_{pd} [and V_{pp}, not shown in Fig. 5(b)] the holes are ''pushed'' toward the peripheral O(2) sites since a hole on O(2) interacts with the charge en_d residing at the copper site and two charges en_{p1} at the two neighboring O(1) sites ($-e$ denotes the electron charge). This has to be compared with twice the Coulomb interaction strength $2en_dV_{pd} + 4en_{p2}V_{pp}$ for a hole on a central O(1) site. Obviously, the energy gain of the hole residing at O(2) is reduced with increasing on-site energy of the side oxygen, that is, with increasing Δ_{pp}. Thus both interactions V_{pd} and V_{pp} must be considered together on an equal footing. We notice that at positive Δ_{pp}, and also for negative values with small absolute values $|\Delta_{pp}|$, the functions $R = R(V_{pd}, \Delta_{pp})$ behave quasilinearly:

$$R \approx R_0 + a_V V_{pd} - b_\Delta \Delta_{pp}, \qquad (4)$$

where $a_V, b_\Delta > 0$. Different values of Δ_{pp} result in a nearly parallel shift of the curves in Figs. 5(a) and 5(b). Both the slope a_V and the coefficient b_Δ depend somewhat on the magnitude of the transfer integrals t_{p1d} and t_{p2d}. Larger transfer integrals imply smaller values of a_V and b_Δ. Notably, the ratio a_V/b_Δ depends much more weakly on the actual value of the Cu-O transfer integral.

In general, larger hybridizations lead to a smoother, more equalized hole distribution. Thus hybridization can be regarded as the ''restoring force'': hindering the shift of the oxygen holes toward the outer oxygens forced by the intersite Coulomb interaction V_{pd} and/or by negative Δ_{pp}. This interplay is most dramatically seen in the t_{pp} dependence of R illustrated in Fig. 6. On going from zero oxygen-oxygen hole transfer to that estimated by the four-band LCAO-LDA derived data (1.15 eV) the value of R changes by about a factor of 2. On the other hand, the result of the seven-band LCAO–LDA fit mentioned above and the frequently used approximation for the transfer integral $t_{pp} \approx 0.5t_{pd}$ suggest a markedly smaller transfer integral $t_{pp} \sim 0.6$ to 0.7 eV. Therefore in our improved parameter sets II and III we use instead of $t_{pp} = 1.15$ eV (set I) 0.65 to 0.75 eV. Such a somewhat reduced t_{pp} value is also helpful in preventing the overestimation of the exchange integrals (see below).

From the intersection of the theoretical R curves with the XAS ratio $R_{XAS} = 1.22$ shown in Fig. 5(b) we found a lower bound for the empirical V_{pd} value at a given Δ_{pp} for fixed remaining parameters in the given set. This results in the empirical constraint Δ_{pp} vs V_{pd} we are searching for, which
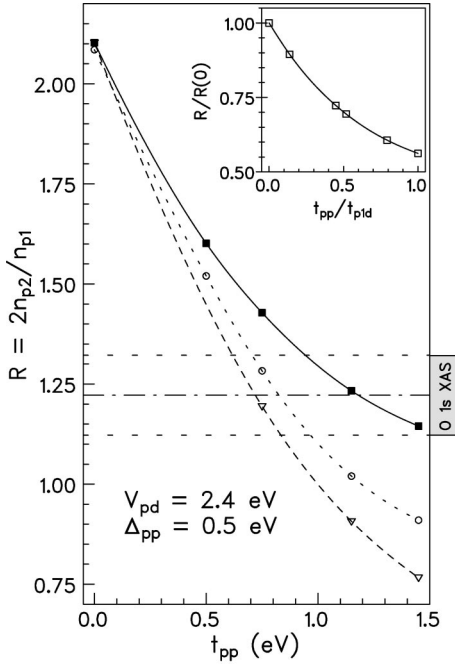
FIG. 6. The relative hole distribution between the two inequivalent oxygen sites $R = 2n_{p2}/n_{p1}$ vs the O(1)-O(2) transfer integral t_{pp} for a typical intersite Coulomb interaction $V_{pd} = 2.4$ eV and the parameter set I shown in Table I. The dashed and dotted curves denote $1/N$ extrapolations to the infinite chain limit for R and n_{p1}, respectively. The inset shows the same dependence of the full line curve plotted in relative units.

is presented in Fig. 7. This dependence is again quasilinear but the coefficients are now less affected by the actual values of the transfer integrals.

Inspection of Fig. 7 clearly demonstrates that $\Delta_{pp} \sim 2$ eV is unlikely because it would result in unreasonably large completely unscreened values of $V_{pd} \sim 6$ to 7 eV;[12,13] pointing formally toward the Kondo limit $V_{pd} \gtrsim t_{pd}$.[21] If V_{pd} is taken by the screened point charge expression $V_{pd} \lesssim 2e^2/(\epsilon a) \sim 2.5$ to 3.7 eV, a screening factor $\epsilon = 2$ to 3 can be estimated. However, further non-NN Coulomb interactions can be lumped into the effective V_{pd}'s (see below).

A further check for the whole parameter set can be obtained by considering the value of the charge transfer gap E_g. The calculated values of E_g obtained from Eq. (3) are listed in Table II. A reasonable agreement with experimental data is achieved for sets II and III.

Summarizing our theoretical analysis so far, the observed hole distribution leads to a clear restriction of the intersite Coulomb interaction to values of $V_{pd} \sim 2$ to 3 eV as visualized in Fig. 7 by the circle indicating the most favored parameter range. This is indeed significantly larger than in the case of layered cuprates, $V_{pd}^{2D} \lesssim 1.2$ eV. Note that the above conclusions are relatively robust with respect to the set of transfer integrals adopted.

The reason for the enhanced Coulomb interaction might be related to reduced screening in quasi-1D compounds as well as to a different extent of the Wannier functions as compared to quasi-2D systems. These effects may also be reflected in the unusual values of the transfer integrals as well as in an enhanced direct ferromagnetic copper-oxygen exchange interaction K_{pd}.
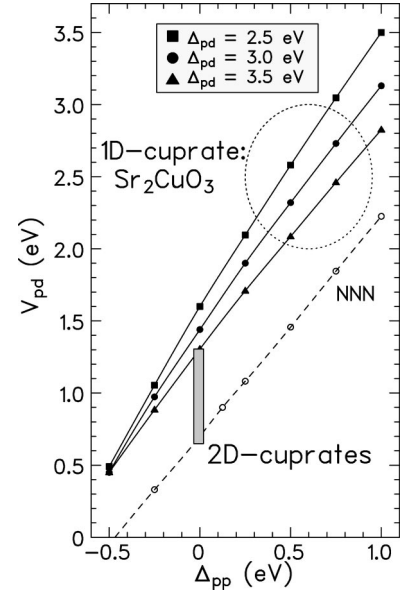

FIG. 7. The empirical relationship between the oxygen on-site energy difference Δ_{pp} and the intersite Coulomb interaction V_{pd}. The curves were obtained using the relative hole distribution R_{XAS} derived from the O 1 s XAS polarization-dependent intensity ratio near 529 to 530 eV (see Fig. 4) using the results of Fig. 5(b). The curve denoted by NNN was obtained including next-nearest-neighbor Coulomb interaction as accounted for in parameter set III (Table I), but with the same R_{XAS} constraint as above. For details see the text. The circle and the box indicate the most favored parameter ranges for Sr_2CuO_3 and the 2D cuprates, respectively.

V. COMPARISON WITH THE SINGLE-BAND EELS DATA ANALYSIS: EVIDENCE FOR STRONG NNN COULOMB INTERACTION?

The recent interpretation of the lowest-lying structures in the EELS data[20] of Sr_2CuO_3 within an effective *single*-band extended ordinary Hubbard model is of interest because there is also an indication of a strongly enhanced NN intersite [i.e., interplaquette (CuO_3 radical) type in our sense]

TABLE II. The charge transfer gap E_g, the oxygen hole ratio $R = 2n_{p2}/n_{p1}$, the antiferromagnetic part of the Heisenberg exchange parameter J, and the effective single-band on-site repulsion $U^{(1B)}$ calculated for the parameter sets shown in Table I and discussed in the text. In parentheses the results of the incremental technique (*) and/or the $1/N$ extrapolations to the infinite chain limit are given. For comparison with Ref. 10 the gap values obtained by exact diagonalization of Cu_4O_{12} clusters are presented for the sets KO1 and KO2.

| | Quantity | | | |
| | E_g | R | J | $U^{(1B)}$ |
Set	(eV)		(meV)	(eV)
KO1	2.43 (1.73*)	1.45 (1.3)	250	3.8
KO2	2.22 (1.53*)	1.34 (1.19)	274	3.6
TM	0.89*	0.93	187	2.06
Set I	2.08 (1.285*,1.5)	1.22	464	4.6
Set II	2.33 (1.85*,1.79)	1.22	270	4.3
Set III	2.23 (1.59*,1.74)	1.33 (1.12)	358	4.4
Experiment	1.7±0.2	1.22±0.1	180 to 260	4.2±0.4

Coulomb interaction $V^{(1B)} \approx 0.8 \pm 0.1$ eV has been found. We remind the reader that in standard mapping procedures from dp models $V^{(1B)} \propto V_{pd}$.[58,21] Comparing the intersite Coulomb contributions to the total ground state energy within the single- and the four-band models, with the aid of the calculated density-density correlation functions and occupation numbers introduced in Sec. II B, we estimate roughly

$$V^{(1B)} \sim \frac{1}{\langle n_l n_{l+1} \rangle_1} [\langle n_d n_{p1} \rangle V_{pd} + \langle n_d(l) n_d(l+1) \rangle V_{dd}$$
$$+ 2\langle n_{p1} n_{p2} \rangle V_{pp} + \langle n_{p1}(l) n_{p1}(l+1) \rangle V_{p1p1}$$
$$+ 2\langle n_{p2}(l) n_{p2}(l+1) \rangle V_{p2p2}]$$
$$\sim n_d n_{p1} V_{pd} + n_d^2 V_{dd} + 2 n_{p1} n_{p2} V_{pp} + n_{p1}^2 \tilde{V}_{p1p1}$$
$$+ 2 n_{p2}^2 \tilde{V}_{p2p2}, \qquad (5)$$

where the NNN Coulomb interactions V_{dd}, V_{pp}, and $\tilde{V}_{pipi}$ ($i=1,2$), have been introduced. Note that these interactions are usually neglected in the overwhelming majority of the ''dp'' literature. In Eq. (5) l denotes the site index of the CuO$_3$ radical unit. For typical parameters in the strongly coupled case we have $\langle n_l n_{l+1} \rangle_1 \approx 0.94$. The first term yields at most $\approx 0.125 V_{pd} = 0.3$ to 0.4 eV. We note that our estimate is very close to the result of $V = 0.17$ eV $= 0.131 V_{pd}$ obtained by Feiner *et al.*[58] for an effective single-band model of the CuO$_2$ plane starting from the standard dp model set with $t_{pd} = V_{pd} = 1.3$ eV.

Returning to the CuO$_3$ chain, we note that the above mentioned empirically twice as large value of $V^{(1B)}$ could be approximately reproduced if at least the second term were taken into account, too. Adopting, for instance, $V_{dd} = 0.85$ eV we arrive at $V^{(1B)} \approx 0.6$ eV for the parameter set III given in Table I. To the best of our knowledge the corresponding plane parameters have not been calculated or measured. An estimate of 0.2 to 0.4 eV for the contribution of the effect of V_{dd} and various V_{pp}'s to $V_{2D}^{(1B)}$ was made in Ref. 21.

To illustrate the effect of the NNN Coulomb interaction we have included in Fig. 7 the relation V_{pd} vs Δ_{pp} for our parameter set III, now with smaller values of V_{pd}, but with $V_{dd} = 0.5 V_{pd}$ and $V_{pp} = V_{pd}/\sqrt{2}$. Fixing in this way the relative magnitudes of all intersite Coulomb interactions, we determined which general scaling factor V_{pd} reproduces $R = 1.22$. This allows a direct comparison with the other curves in Fig. 7. Note that for 0.75 eV $\leqslant \Delta_{pp} \leqslant 1$ eV the values obtained for the NNN set approach the favored parameter range of sets I and II denoted by the circle. This shows that, in principle, the NNN Coulomb interactions are of minor direct importance for analysis of the O 1s XAS data as presented here. They can be included implicitly in the on-site energies of reduced effective NN models. For instance, the oxygen hole ratio R between peripheral and central oxygen atoms is affected by the actual value of V_{dd} via a redistribution of charge between Cu and O(1) sites. Nevertheless, the analysis of Eq. (6) suggests that, in a deeper microscopic description of *other* experiments, the adequate explicit treatment of further non-NN Coulomb interactions such as V_{dd} may be crucial.
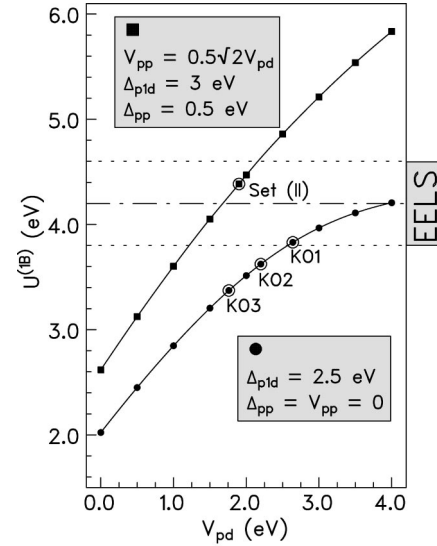

FIG. 8. The effective on-site Coulomb repulsion $U^{(1B)}$ according to Eq. (A1) of the extended single-band extended Hubbard model vs intersite Coulomb interaction V_{pd} of the four-band dp extended Hubbard model adopted in the present paper. The upper curve contains one of the parameter sets (set II) adopted in the present paper. The lower curve covers the parameter sets proposed by Okada and Kotani (Ref. 10) [$V_{pd} \sim (0.2-0.3) U_d$ denoted by KO1 to KO3 and marked by circles].

Note that the empirical value of the effective on-site interaction $U^{(1B)}$ for the extended single-band Hubbard model derived from the EELS data[20] of 4.2 ± 0.4 eV significantly exceeds $\Delta_{p1d} = 3 \pm 0.5$ eV for most of the parameter sets we have considered, whereas in the standard 2D case usually $\Delta_{pd} \approx U^{(1B)} \pm 0.5$ eV holds.[59] We ascribe this effect to the enhanced intersite Coulomb interaction under consideration. Enhancement of U^{1B} due to increasing V_{pd} has been mentioned in the 2D case, for instance, by Feiner *et al.*[58] and Simon *et al.*[61] in related single-band models.

By using Eq. (A1) we estimate values of $U^{(1B)}$ for the three parameter sets KO and our sets derived from the XAS data. The relation $U^{(1B)}$ as a function of V_{pd} is presented in Fig. 8. One realizes that the KO1 set with the largest V_{pd} value just reaches the lower bound of the $U^{(1B)}$ region derived from the EELS data whereas the same parameter set gives an R value greater than that derived from the present XAS data. The sets KO2 and KO3 yield smaller $U^{(1B)}$ values compared, for example, with set II, which is well within the EELS error bars. In contrast to $V^{(1B)}$, here by definition [compare Eqs. (5) and (A1)] the effect of V_{dd} on $U^{(1B)}$ is implicit only via its influence on the correlation functions.

Finally, for completeness we consider briefly a parameter set proposed recently for Sr$_2$CuO$_3$ by Mizuno *et al.*[49] to explain the enhanced superexchange J in corner-sharing 1D cuprates. This set is similar to the TM set discussed above, with now somewhat larger but nevertheless still slightly reduced transfer integrals ($t_{p1d} = 1.16$ eV, $t_{p2d} = 1.09$ eV, $t_{pp} = 0.49$ eV), with a standard charge transfer energy $\Delta_{pd} = 3.1$ eV, but with *negative* $\Delta_{pp} = -0.6$ eV, with standard on-site Coulomb interactions $U_d = 8.5$ eV and $U_p = 4.1$ eV, and again *without* any intersite Coulomb interaction. The on-site energies are derived within the point charge approximation from a Madelung potential analysis.[52] Naturally, a nega-

tive Δ_{pp} together with small t_{pp} and $V_{pd}=0$ would be helpful to satisfy the XAS constraint for R [compare Eq. (5) and Figs. 4–6]. The small transfer integrals together with the small direct ferromagnetic exchange interaction K_{pd} $=0.05$ eV reveal only a moderately enhanced exchange integral of $J=170$ meV, to be compared with the experimental value in the range of 180 to 260 meV. But the effective onsite energy $U^{1B}\approx 4.2\pm 0.4$ eV seen in the EELS data would be significantly underestimated ($U^{1B}<3$ eV) and of course no excitonic effects can be explained by definition since $V^{(1B)}\equiv 0$ [compare Eq. (5)]. Despite the obvious fact that the Hamiltonian parameter may change if new interactions are added,[39,62] we argue that the oxygen on-site energies calculated in Refs. 49, 52, and 39 are affected by the ionic point charge approach adopted, which probes only the Madelung potential at the site under consideration. In contrast, the extended and strongly anisotropic $2p$ Wannier functions do probe the crystal field, i.e., they feel the anisotropic surroundings of the site. According to our experience with various cuprate band structures, such a crystal field effect may result in oxygen $2p$ on-site energy splittings on the order of up to 2 eV. [In particular, for just this reason in addition to the small interoxygen transfer integrals, the O(2) $2p_x$ and O(1) $2p_y$ orbitals that enter the seven-band model mentioned above can be ignored in the present XAS analysis.] Hence, crystal field corrections to the point charge model derived on-site energies on the order of 0.5 to 1 eV cannot be excluded. Because of the Sr^{2+} ion residing above the O(2) site, a positive correction is expected. As a result, within a more realistic description for an effective model that ignores the intersite Coulomb interaction $\Delta_{pp}\sim -0.1$ to 0.4 eV can be expected. The remaining difference of 0.4 to 0.8 eV is ascribed to the mapping between extended and simple Hubbard Hamiltonians.[62]

In any case, we emphasize once again that our estimate of strongly enhanced intersite Coulomb interaction rests on the validity of the assumptions of a sufficiently positive Δ_{pp} value and large transfer integrals, and/or the validity of the one-band analysis of the EELS data given in Ref. 20. To summarize, the XAS data and the value of $U^{(1B)}$ derived from the EELS data can be nearly equally well described within the NN and the NNN approximations, whereas the $V^{(1B)}$ value is strongly underestimated in the NN approximation. The NNN interaction included in parameter set III yields a reasonable description of almost all available experimental data (see Table II), except for the overestimation of the J value.[64] On increasing the on-site repulsion on oxygen sites U_p up to 6 eV, the magnitude of J can be reduced to a value of 338 meV as mentioned in Table II. (Note that the single-band parametrization derived from the EELS data results in a similarly enhanced value of $J=356$ meV.) In our opinion the solution of this challenging problem might be found in the inclusion of additional ferromagnetic interactions (as well as the enhanced transfer integrals and the intersite Coulomb interaction) that are neglected in Eq. (1), such as K_{pd} and K_{pp} (see, e.g., Refs. 12 and 16). Due to the spin-charge separation characteristic for 1D systems, both spectroscopies (XAS and EELS) are expected to be insensitive to such interactions.[20] Of course, other orbitals and interactions outside the four-band extended Hubbard model might affect the value of the exchange parameter J.[65] Finally,

we emphasize that it was not the aim of the present approach to give a full quantitative description of either the magnetic susceptibility data or the EELS data. Rather, only the likely directions for the inclusion of further necessary interactions have been outlined. Thus a direct simulation of the EELS data within a multiband model remains a challenging problem worth being tackled.

VI. COMPARISON WITH THE XAS DATA OF THE DOUBLE-CHAIN COMPOUND $SrCuO_2$

It is instructive to compare the unoccupied electronic structure of Sr_2CuO_3 with that of the related double-chain compound $SrCuO_2$, which has been studied recently.[23] The two inequivalent oxygen sites of the Cu_2O_4 double chain are reflected in the polarization-dependent x-ray absorption spectra in an analogous manner to that discussed above for Sr_2CuO_3. This results in a double-peaked UHB derived feature for $\mathbf{E}\|\mathbf{b}$ (in the axis notation of the present paper) with an energy separation of the two peaks of 0.5 eV. Our assignment of the different peaks in Sr_2CuO_3 to the two oxygen sites is thus fully consistent with the double-chain result, relating the energetically lower-lying UHB derived feature to the outer oxygen atoms of the chain.

The peak positions ascribed to transitions into $2p_y$ states within the notation adopted here occur for both compounds at nearly the same energy: 529.1 eV mentioned above for Sr_2CuO_3 in comparison with 529.3 eV for the low-energy peak of $SrCuO_2$. The transitions into $2p_x$ states occur at 529.6 eV for the former compound to be compared with 529.8 eV for the double-chain compound. Both differences are comparable with the enhancement of the optical gap by ~ 0.3 eV in the double-chain compound deduced from the low-energy maxima of the optical conductivity.[66]

Finally, we briefly compare the single CuO_3 chain with the Cu_2O_4 double chain from the theoretical point of view. We note that the double chain (DC) to a first crude approximation can be treated in a similar (but asymmetric) single-chain (SC) model to that given above, if first of all the symmetry between the two peripheral oxygen sites "O(2a)" and "O(2b)" in the single chain is lifted [i.e., we formally split the double chain into two equivalent single chains: a central oxygen of the double chain now becomes a peripheral oxygen "O(2b)" of the corresponding asymmetric single-chain problem]. The consequences of possible slight differences between t_{dp2a} and t_{dp2b} and between t_{p1p2a} and t_{p1p2b} are briefly discussed below. The electron (hole) transfer processes related to the transfer integrals $t_{pp,\|}\sim 0.5 t_{pp}$, and other small interactions are neglected.

Thus considering such an asymmetric single subchain of the double chain, one can adopt the following expressions for the on-site energies of the central oxygen O(1) and the two peripheral oxygen sites O(2a) and O(2b) [we recall that the O(2b) site was a central oxygen site in the double chain before its splitting]:

$$\varepsilon_{p1}\rightarrow\varepsilon_{p1}^{(SC)}+n_d\tilde{V}_{pd}+n_{p2b}U_{2p1},$$

$$\varepsilon_{p2a}\rightarrow\varepsilon_{p2}^{(SC)},$$

$$\varepsilon_{p2b}\rightarrow\varepsilon_{p2}^{(SC)}+2n_d\tilde{V}_{pd}+n_{p1}U_{2p1}. \tag{6}$$

Now the Cu and two of the three O hole expectation numbers, n_d, n_{p1}, and n_{p2b}, respectively, entering Eq. (6) must be found self-consistently. In Eqs. (6) $\tilde{V}_{pd} < V_{pd}$ denotes the intersite Coulomb interaction between perpendicular (non-σ) oriented oxygen orbitals and $U_{p2p1} = U_p - 2K < U_p$ is the interorbital on-site Coulomb repulsion. Here $K > 0$ denotes the Hund's rule coupling (the corresponding magnetic spin flip term that is important for magnetic properties has been neglected). In our estimates given below we will adopt $K/U_p \approx 0.15$.[49,39] Thus we take $U_{p1p2} = 3$ eV as a representative estimate.

Analysis of the XAS data of the double-chain compound $SrCuO_2$ reveals that nearly the same total number of holes reside in $2p_y$ states as in the single-chain case:

$$R_{SC} \sim R_{DC} = (n_{p2a} + n_{p2b})/n_{p1} \approx 1.16.$$

Apparently, the relative number of holes at the outer and inner oxygen sites in the $2p_y$ states directly measures the asymmetry of the problem:

$$\eta = n_{p2a}/n_{p2b} \approx 1.19. \tag{7}$$

In other words, $\eta > 1$ suggests $\varepsilon_{p2b} > \varepsilon_{p2a}$. Then, according to Eqs. (6) this significant asymmetry should be related to (i) the two additional Cu sites surrounding a $2p_y$ hole at the inner oxygen site O(1) compared with one Cu site for a $2p_y$ hole at the outer O(2) sites in $SrCuO_2$ as well as in Sr_2CuO_3, and most importantly (ii) the presence of the interorbital (on-site) Coulomb repulsion $U_{p1p2} < U_p$ at the O(1) sites, where now in contrast to the O(2) sites two orbitals with $2p_x$ and $2p_y$ character, respectively, are involved. The experimental value of R_{DC} mentioned above can be reproduced by parameter sets closely related to those of the single chain, whereas for symmetric transfer integrals the calculated η value comes out slightly too large ($\eta_{theor} \approx 1.35$ to 1.4). However, taking into account the slightly buckled ''backbone'' structure of $SrCuO_2$,[67] $t_{p1p2b} > t_{p1p2a}$ can be expected. Similarly, from the different Cu-O distances ($d_{Cu-O(1)} \approx 1.91$ Å compared with $d_{Cu-O(2)} \approx 1.93$ Å) slightly different values of the transfer integrals t_{dp2a} and t_{dp2b} are suggested. In addition, the shorter Cu-O distances compared with Sr_2CuO_3 ($d_{Cu-O} = 1.95$ Å) also suggest further enhanced transfer integrals. All these effects are helpful in decreasing the former theoretical value of the anisotropy parameter η toward the experimental value. A quantitative analysis will be given elsewhere in connection with a detailed band structure analysis of $SrCuO_2$.

As the hole distribution of both compounds shows a pronounced similarity, the specific magnetic frustration present in $SrCuO_2$ seems to be of no direct relevance for the charge distribution. Again, this might be a consequence of the spin-charge separation in both the systems.[1,2] To summarize, the pronounced similarity and even the remaining slight differences in the electronic properties of Sr_2CuO_3 and $SrCuO_2$ can be understood in the framework of our slightly generalized four-band dp models.

VII. SUMMARY

To summarize our results, direct experimental information on the character and symmetry of the intrinsic holes in a CuO_3 chain has been obtained by polarization-dependent x-ray absorption spectroscopy. The intrinsic holes predominantly occupy orbitals in the plane of the CuO_4 plaquettes as in the case of the undoped parent compounds of the high-T_c superconductors.

Examining various proposed parameter sets, we have shown the following.

(i) Combined with an exact diagonalization study of a Cu_6O_{18} cluster, the polarization-dependent O $1s$ XAS intensities provide a clear constraint on the values of both the intersite Coulomb interaction V_{pd} and the difference of the on-site energies Δ_{pp} for the two inequivalent oxygen sites. Note that other related spectroscopies such as Cu $2p$ XPS are not sensitive to the precise values of these parameters.[10]

(ii) The intersite Coulomb interaction cannot be ignored in the interpretation of the O $1s$ XAS data. If one attempts to set V_{pd} to zero, unusually low on-site energies of the outer oxygen sites O(2) must be adopted to reproduce the experimentally observed oxygen hole ratio $R_{XAS} = 2n_{p2}/n_{p1} \approx 1.22$.

(iii) For a feasible value of the oxygen on-site energy difference $\Delta_{pp} \sim 0.5$ eV, a strongly enhanced nearest-neighbor intersite Coulomb interaction of the order of 2 to 3 eV is required to reproduce R_{XAS}. Comparison with the single-band analysis of the EELS data from the same system[20] points to the non-negligible role of at least a second-neighbor Coulomb interaction, which has been widely neglected so far in the literature. The oxygen hole ratio R is markedly sensitive also to the value of the oxygen-oxygen transfer integral t_{pp}. Thereby, unusually large values of t_{pp} (exceeding 1 eV) can be excluded on the basis of the XAS data.

(iv) Combining the present XAS analysis with the results of other spectroscopies (EELS, XPS, optical data) and magnetic susceptibility measurements we have refined dp model parameter sets for Sr_2CuO_3. We found several significant deviations from the commonly accepted sets for the related layered cuprates: for the 1D case enhanced intersite Coulomb interactions and transfer integrals as well as a slightly reduced difference of the in-chain oxygen-copper on-site energies are necessary.

(v) The unoccupied electronic structure of the single- and double-chain compounds realized in Sr_2CuO_3 and $SrCuO_2$ is found to be rather similar. Small differences can be ascribed to additional interorbital U_{pp} and intersite Coulomb interaction $\tilde{V}_{pd} \sim 2.5$ eV in $SrCuO_2$ caused by the specific structure of its double chains. The latter effects are somewhat weakened by the slight asymmetry of the transfer integrals.

Since our results point to significantly enhanced V_{pd} values compared to those for typical layered cuprates, the highly doped CuO_3 chains of the $RBa_2CuO_3O_7$ family analyzed within a slightly modified ''2D'' derived parameter set should be reanalyzed with respect to the modified parameters obtained here. In this context the recently reported charge instability in the CuO_3 chains of $PrBa_2Cu_3O_7$ by Grévin *et al.*[68] is of special interest since it is well known that charge density wave type instabilities can be driven or strongly supported by large intersite Coulomb interactions.[69]

Our approach represents a good starting point for the analysis of other chain cuprate materials with inequivalent

oxygen sites such as the double-chain compound $SrCuO_2$ and the ladder compounds.

APPENDIX: ESTIMATE OF THE EFFECTIVE ON-SITE PARAMETER FOR THE SINGLE-BAND MODEL

Since the low-energy EELS measurements of the dynamical dielectric response of Sr_2CuO_3 have been analyzed within the single-band extended Hubbard model,[20] it is desirable to relate the effective on-site repulsion $U^{(1B)}$ to the parameters of the four-band pd model discussed here. To illustrate this point we consider [analogously to the estimate of V^{1B} (Eq. 5)] the following quantity:

$$u = D_{d,2}U_d + (2D_{p2,2} + D_{p1,2})U_p + (\langle n_d n_{p1}\rangle_2$$
$$+ 2\langle n_d n_{p2}\rangle_2)V_{pd} + 2\langle n_{p1} n_{p2}\rangle_2 V_{pp} + \langle n_{p2a} n_{p2b}\rangle_2 \widetilde{V}_{p2p2}$$
$$+ (n_{p1,2} - n_{p1,2}^{(0)})\Delta_{p1d} + 2(n_{p2,2} - n_{p2,2}^{(0)})(\Delta_{pp} + \Delta_{p1d}),$$
$$(A1)$$

which serves as a rough but useful interpolation formula $u \approx U^{(1B)}$ at arbitrary parameters. Here the double occupancies $D_{i,2}$ ($i = d, p_1, p_2$), the correlation functions $\langle \cdots \rangle_2$, and the occupation numbers $n_{i,2}$ entering Eq. (A1) have been calculated for the case of *two* holes per unit cell, and $\langle n_{p2a} n_{p2b}\rangle$ denotes the correlation function between the two equivalent peripheral oxygens ''O(2a)'' and ''O(2b)'' residing on the same chain unit. The occupation numbers with the superscript (0) are calculated by setting the Coulomb interactions to zero, i.e., in the one-particle limit.

*Author to whom all correspondence should be addressed. Email address: drechsler@ifw-dresden.de

†On leave from Institute of Physics, Academy of Sciences of the Czech Republic, Prague.

‡Present address: Department of Physics, University of California, Davis, CA, 95616.

[1] C. Kim, A.Y. Matsuura, Z.-X. Shen, N. Motoyama, H. Eisaki, S. Uchida, T. Tohyama, and S. Maekawa, Phys. Rev. Lett. **77**, 4054 (1996); C. Kim, Z.-X. Shen, N. Motoyama, H. Eisaki, S. Uchida, T. Tohyama, and S. Maekawa, Phys. Rev. B **56**, 15 589 (1997).

[2] H. Fujisawa, T. Yokoya, T. Takahashi, S. Miyasaka, M. Kibune, and H. Takagi, Solid State Commun. **106**, 543 (1998).

[3] E. Dagotto and T.M. Rice, Solid State Commun. **271**, 618 (1996).

[4] T. Ami, Phys. Rev. B **51**, 5994 (1995).

[5] N. Motoyama, H Eisaki, and S. Uchida, Phys. Rev. Lett. **76**, 3212 (1996).

[6] K.M. Kojima, Y. Fudamoto, M. Larkin, G.M. Luke, J. Merrin, B. Nachumi, Y.J. Uemura, N. Motoyama, H. Eisaki, S. Uchida, K. Yamada, Y. Endoh, S. Hosoya, B.J. Sternlieb, and G. Shirane, Phys. Rev. Lett. **78**, 1787 (1997).

[7] Recent angle resolved photoemission data analysis given by Fujisawa *et al.* (Ref. 2) yields somewhat smaller J values of 130 to 160 meV from the width of the spinon dispersion.

[8] J. Zaanen, G.A. Sawatzky, and J.W. Allen, Phys. Rev. Lett. **55**, 418 (1985).

[9] K. Maiti, D.D. Sarma, T. Mizokawa, and A. Fujimori, Europhys. Lett. **37**, 359 (1997); Phys. Rev. B **57**, 1572 (1997).

[10] K. Okada and A. Kotani, J. Phys. Soc. Jpn. **66**, 341 (1997).

[11] H. Eskes, G. Sawatzky, and L. Feiner, Physica C **41**, 424 (1989).

[12] E.B. Stechel and D.R. Jennison, Phys. Rev. B **38**, 4632 (1988).

[13] Han Rushan, C.K. Chew, K.K. Phua, and Z.Z. Gan, Phys. Rev. B **39**, 9200 (1989).

[14] A.K. McMahan, J.F. Anett, and R.M. Martin, Phys. Rev. B **42**, 6268 (1990).

[15] M.S. Hybertsen, M. Schlüter, and N.E. Christensen, Phys. Rev. B **39**, 9028 (1989).

[16] M.S. Hybertsen, E.B. Stechel, W.M.C. Foulkes, and M. Schlüter, Phys. Rev. B **45**, 10 032 (1992).

[17] A.A. Aligia and J. Garcés, Phys. Rev. B **49**, 524 (1994).

[18] M.E. Simón and A.A. Aligia, Phys. Rev. B **53**, 15 327 (1996).

[19] M.E. Simón, A.A. Aligia, C.D. Batista, E.R. Gagliano, and F. Lema, Phys. Rev. B **54**, R3780 (1996).

[20] R. Neudert, M. Knupfer, M.S. Golden, J. Fink, W. Stephan, K. Penc, N. Motoyama, H. Eisaki, and S. Uchida, Phys. Rev. Lett. **81**, 657 (1998).

[21] H.-B. Schlüter and A.J. Fedro, Phys. Rev. B **45**, 7588 (1992).

[22] H. Rosner, H. Eschrig, R. Hayn, S.-L. Drechsler, and J. Málek, Phys. Rev. B **56**, 3402 (1997).

[23] M. Knupfer, R. Neudert, M. Kielwein, S. Haffner, M.S. Golden, G. Krabbes, J. Fink, C. Kim, Z.-X. Shen, M. Merz, N. Nücker, S. Schuppler, N. Motoyama, H. Eisaki, S. Uchida, Z. Hu, M. Domke, and G. Kaindl, Phys. Rev. B **55**, R7291 (1997).

[24] Ch. Krüger, W. Reichelt, A. Almes, U. König, H. Oppermann, and H. Scheler, J. Solid State Chem. **96**, 67 (1992).

[25] M. Domke, T. Mandel, A. Puschmann, C. Xue, D.A. Shirley, G. Kaindl, H. Petersen, and P. Kuske, Rev. Sci. Instrum. **63**, 80 (1992).

[26] A core-level excitation whose absorption coefficient is small compared to the total absorption, as in the case for the O 1s edge, leads to a very poor signal-to-background ratio in TEY, but has the distinct advantage that self absorption effects in the FY mode remain small. The situation is just reversed in the case of the relatively strong Cu 2p absorption.

[27] L.H. Tjeng, C.T. Chen, and S.W. Cheong, Phys. Rev. B **45**, 8205 (1992).

[28] J. Jaklevic, J.A. Kirby, M.P. Klein, and A.S. Robertson, Solid State Commun. **23**, 679 (1977); L. Tröger, D. Arvanitis, K. Baberschke, H. Michaelis, U. Grimm, and E. Zschech, Phys. Rev. B **46**, 3283 (1992).

[29] J. Fink, N. Nücker, E. Pellegrin, H. Romberg, M. Alexander, and M. Knupfer, J. Electron Spectrosc. Relat. Phenom. **66**, 395 (1994).

[30] Compared with Cu $3d$ final states the probability for transitions into unoccupied Cu $4s$ orbitals is smaller by a factor of 20 [B.K. Teo and P.A. Lee, J. Am. Chem. Soc. **101**, 2815 (1979)].

[31] S.-L. Drechsler, J. Málek, and H. Eschrig, Phys. Rev. B **55**, 606 (1997); S.-L. Drechsler, J. Málek, S. Zališ, and K. Rościszewski, *ibid.* **53**, 11 328 (1996).

[32] A. Oleś and M. Grzelka, Phys. Rev. B **44**, 9531 (1991).

[33] Some remaining possible uncertainties in the knowledge of the hopping parameters [due to difficulties in separating in the LDA analysis the electrons to be described explicitly in multiple-band extended Hubbard models from other valence (pd) electrons included implicitly in the core parameters] look less dramatic compared with the corrections ~ 0.2 to 0.5 eV for the transfer integrals due to medium or strong intersite Coulomb interactions in Hartree-Fock type band structures (see Refs. 34, 32, 35, and 13). In this context the empirical reliability of the LDA derived transfer integrals found for various layered cuprates is noteworthy (Ref. 36).

[34] V.J. Emery, Phys. Rev. Lett. **58**, 2794 (1987).

[35] L.F. Mattheiss, Phys. Rev. Lett. **58**, 1028 (1987). In this work $t_{pd} \approx 1.6$ eV has been estimated from the calculated band structure of La_2CuO_4 to be compared with 1.5 eV obtained in Ref. 13 from a straightforward calculation approximating the Wannier functions by orbital wave functions.

[36] H. Rosner, Ph.D. Thesis, University of Technology, Dresden, 1999; H. Rosner, R. Hayn, and J. Schulenburg, Phys. Rev. B **57**, 13 660 (1998). For instance, $t_{pd} = 1.33$ eV and 1.43 eV as well as $t_{pp} = 0.71$ eV and 0.81 eV have been obtained for $Sr_2CuO_2Cl_2$ and $Ba_2Cu_3O_4$, respectively.

[37] N. Kothekar, K.F. Quader, and D.W. Allender, Phys. Rev. B **51**, 5899 (1995).

[38] T. Tohyama and S. Maekawa, J. Phys. Soc. Jpn. **60**, 53 (1991).

[39] Y. Mizuno, T. Tohyama, S. Maekawa, T. Osafune, N. Motoyama, H. Eisaki, and S. Uchida, Phys. Rev. B **57**, 5326 (1998).

[40] J. Málek, K. Kladko, and S. Flach, Phys. Rev. B **59**, R5273 (1999); Pis'ma Zh. Éksp. Teor. Fiz. **67**, 994 (1998) [JETP Lett. **67**, 1052 (1998)]; cond-mat/9710112 (unpublished) modified here for the four-band model under consideration.

[41] To check the accuracy of the QMC calculation we compared the corresponding calculations for $(CuO_3)_4$ and $(CuO_3)_6$ clusters which can still be handled by our exact diagonalizations: deviations in the occupation numbers of the order of only 0.4% have been detected (Refs. 42 and 43). Therefore we believe that the corresponding QMC results for $N = 16$ (which corresponds to 64 sites in total) can be trusted as a good approximation for the thermodynamic infinite chain limit (ICL) of interest. Furthermore, it turned out that these clusters belong to two different subclasses, $N = 4m$ and $N = 4m - 2$, for which the calculated occupation numbers and the total energies tend monotonically very fast to the common infinite chain limit $N \to \infty$ from above and below, respectively, as $\sim N^{-2}$. For typical parameters we found that quantities obtained for the $N = 6$ cluster are already surprisingly close to the QMC ICL. The magnitude of the finite size effects depends strongly on the value of the transfer integrals. For instance, in the worst case of strongly enhanced transfer integrals we have $n_d(N=\infty) \approx 0.7 n_d(N=6) + 0.3 n_d(N=4)$. Since usually the absolute values of the occupation numbers from $N = 6$ clusters obtained by the exact diagonalization studies

differ by only a few percent from the QMC ICL estimates, we present in most cases only the former quantities.

[42] C. Waidacher, Ph.D. thesis, University of Technology, Dresden, 1999.

[43] S.-L. Drechsler, J. Málek, H. Rosner, R. Neudert, M.S. Golden, M. Knupfer, J. Fink, H. Eschrig, C. Waidacher, and R. Hetzel, J. Low Temp. Phys. **117**, 407 (1999).

[44] In the evaluation of the spectral weight, different matrix elements for transitions into Cu $3d_{xy}$ and Cu $3d_{3z^2-r^2}$ states were taken into account.

[45] S. Haffner, R. Neudert, M. Kielwein, M. Knupfer, M.S. Golden, K. Ruck, G. Krabbes, J. Fink, H. Rosner, R. Hayn, H. Eisaki, S. Uchida, Z. Hu, M. Domke, and G. Kaindl, Phys. Rev. B **57**, 3672 (1998).

[46] Thus small features with a total weight of a few percent seen in the XAS spectral density above the main peak have been neglected because it is difficult to separate them from the additional transitions mentioned in the text. Their contribution to the intensity is within the experimental error bars of the main peak.

[47] Y.J. Shin, E.D. Manova, J.M. Dance, P. Dordor, J.C. Grenier, E. Marquestaut, J.P. Doumere, M. Pouchard, and P. Hagenmuller, Z. Anorg. Allg. Chem. **616**, 201 (1992).

[48] K. Maiti, Ph.D. thesis, University of Bangalore, 1998.

[49] Y. Mizuno, T. Tohyama, and S. Maekawa, Phys. Rev. B **58**, R14 713 (1998).

[50] H. Rosner *et al.* (unpublished). In order to illustrate the large sensitivity of the O $1s$ levels to the actual crystal field, we mention that for the apical oxygen O(4) [which corresponds to O(2) of Sr_2CuO_3] and the chain oxygen atoms O(1) of the closely related high-T_c superconductors $YBa_2Cu_3O_7$ and $YBa_2Cu_4O_8$ with CuO_3 chains and CuO_2 double chains, respectively, calculated shifts of the O $1s$ binding energy within the LDA of 0.65 eV and 2.14 eV for O(4) and O(1) have been reported in Ref. 51. The ionic point charge models yield too large energy differences between nonequivalent sites. This flaw is usually corrected by introducing *ad hoc* screening factors ϵ. In Refs. 52, 39, and 49 $\epsilon = 3.5$ and 3.3 have been adopted for layered and chain cuprates, respectively. Since for core electrons the effect caused by the real charge distribution of extended nonpoint charges in the surroundings of the core sites is less dramatic, it can be described by smaller "screening factors."

[51] J. Yu, K.T. Park, and A.J. Freeman, Physica C **172**, 467 (1991).

[52] Y. Ohta, T. Tohyama, and S. Maekawa, Phys. Rev. B **43**, 2968 (1991).

[53] N. Nücker, E. Pellegrin, P. Schweiss, J. Fink, S.L. Molodtsov, C.T. Simon, G. Kaindl, W. Frentrup, C. Thomsen, A. Erb, and G. Müller-Vogt, Phys. Rev. B **51**, 8529 (1995).

[54] M. Merz, N. Nücker, E. Pellegrin, S. Schweiss, S. Schuppler, M. Kielwein, M. Knupfer, M.S. Golden, J. Fink, V. Chakarian, Y.U. Idzerda, and A. Erb, Phys. Rev. B **55**, 9160 (1997).

[55] A. Krol, Z.-H. Ming, Y.H. Kao, N. Nücker, G. Roth, G.C Smith, K.T. Park, J. Yu, A.J. Freeman, A. Erb, G. Müller-Vogt, J. Karpinski, E. Kaldis, and K. Schönmann, Phys. Rev. B **45**, 2581 (1992); (unpublished).

[56] R. Neudert, H. Rosner, S.-L. Drechsler, M. Kielwein, M. Sing, Z. Hu, M. Knupfer, M.S. Golden, J. Fink, N. Nücker, M. Merz, S. Schuppler, N. Motoyama, H. Eisaki, S. Uchida, M. Domke, and G. Kaindl, Phys. Rev. B **60**, 13 413 (1999).

[57] A.A. Aligia, E.R. Gagliano, and P. Vairus, Phys. Rev. B **52**, 13 601 (1995).

[58] L.F Feiner, J.H. Jefferson, and R. Raimondi, Phys. Rev. B **53**, 8751 (1996).

[59] An unusually large on-site repulsion $U^{(1B)} = 5.3 \pm 0.5$ eV at $\Delta_{pd} = 3.6$ eV derived from a cluster mapping given in Ref. 60 was chosen by the authors to describe accurately the effective exchange integral without simultaneous consideration of the charge transfer gap E_g. Therefore later on, in Ref. 16, the reduced value $U^{(1B)} = 4.1$ eV was recommended as more appropriate for description of the XAS problem.

[60] M. Hybertsen, E.B. Stechel, M. Schlüter, and D.R. Jennison, Phys. Rev. B **41**, 11 068 (1990).

[61] M.E. Simon, M. Baliña, and A.A. Aligia, Physica C **206**, 297 (1993).

[62] The necessity of making significant quantitative corrections/renormalizations to/of the $2p$ oxygen on-site energies derived in Refs. 52 and 49 if a standard parameter set is used, can be illustrated for the well-studied apical oxygen problem in YBa$_2$Cu$_3$O$_7$. For instance, according to Refs. 59 and 63 its on-site energy ε_{apex} is crucial for the stability of the Zhang-Rice singlet and in this way for high T_c. To avoid such instabilities ε_{apex} should be higher than 6 to 8 eV above the planar Cu(2) $3d_{x^2-y^2}$ level (Ref. 63). However, the value within the point charge model given in Refs. 49 and 59 reads $\varepsilon_{apex} \approx 2.8$ eV $+1$ eV$= 3.8$ eV, where the former value stands for the plane Δ_{pd}. On adopting even a somewhat higher $\Delta_{pd} = 4$ eV, ε_{apex} should be shifted upward by at least 1 eV. In addition we note that in a rigorous sense the matrix elements of any Hamiltonian should be determined without counting twice the electrons (holes) to be described by it. For the single-chain problem under consideration this means that the electrostatic potential caused by the Cu^{2+} ions along the chain entering the 3D Madelung calculations should be replaced by a potential of Cu^{1+} ions in accordance with the O$|2p^6\rangle$ Cu$|3d^{10}\rangle$ vacuum state of the pd model. As a result one arrives (within the infinite chain limit for a proper point charge model with intersite Coulomb interactions for Sr$_2$CuO$_3$) at a large correction of $+4.1$ eV to the Madelung potential difference of about -2 eV for the two nonequivalent oxygen atoms. From all these considerations we would expect $\Delta_{pp} \geq 0.5$ eV in qualitative agreement with our suggestion shown in Fig. 7.

[63] R. Raimondi, J.H. Jefferson, and L.F. Feiner, Phys. Rev. B **53**, 8774 (1996).

[64] Notice the significant finite size effect for the J value which follows from our much larger Cu$_6$O$_{18}$ cluster: $J = 274$ meV (see Table II). We ascribe this to the enhanced hole delocalization naturally favoring the superexchange. The overestimation of the experimental value could be at least partially explained by the neglect of two ferromagnetic spin flip terms in the dp Hamiltonian [the last two terms in Eq. (1) in Ref. 16]. Keeping this in mind along with the large experimental uncertainty of the total J_{tot} value, we regard an antiferromagnetic contribution $J_{AF} \sim 300 \pm 40$ meV as still being in accord with the currently available experimental data $J \sim 215 \pm 40$ meV. The calculated charge gap values E_g are in agreement with the strong low-energy peak of the optical conductivity reported in Ref. 10. Taking into account the expected finite size effects for E_g and R, the set KO3 with $V_{pd} = 1.76$ eV can also be excluded. Thus, adopting such an otherwise standard parameter set, we would arrive at $V_{pd} \approx 2.2$ eV.

[65] F. Barriquand and G. Sawatzky, Phys. Rev. B **50**, 16 649 (1994).

[66] H. Yasuhara and Y. Tokura (unpublished).

[67] Y. Matsushita, Y. Oyama, M. Hasegawa, and H. Takei, J. Solid State Chem. **114**, 289 (1994).

[68] B. Grévin, Y. Berthier, G. Collin, and P. Mendels, Phys. Rev. Lett. **80**, 2405 (1998).

[69] J.E. Hirsch, in *Low-dimensional Conductors and Superconductors*, Vol. 155 of *NATO Advanced Study Institute, Series B: Physics*, edited by D. Jerome and L.G. Caron (Plenum Press, New York, 1989), pp. 71–86.

[70] Following our convention, the chain lies along the **a** direction and the **c** direction is perpendicular to the planar CuO$_4$ plaquettes (see Fig. 1).